Surface Forces at Restricted Equilibrium, in Solutions Containing Finite or Infinite Semiflexible Polymers

Jan Forsman*

Theoretical Chemistry, Chemical Centre, P.O. Box 124, S-221 00 Lund, Sweden

Clifford E. Woodward†

School of Physical Environmental and Mathematical Sciences, University College, University of New South Wales, Building 22, Australian Defence Force Academy, Canberra ACT 2600, Australia

Received May 25, 2007; Revised Manuscript Received August 22, 2007

ABSTRACT: We use density functional theory to investigate how the presence of polymers influence the interactions between adsorbing or nonadsorbing flat surfaces, forming a slit geometry. The study is primarily made under "restricted equilibrium" conditions, i.e., below a threshold separation, the chains are allowed to equilibrate conformationally between the surfaces, but they are unable to diffuse into or out from the slit. This is believed to be a reasonable model for commonly encountered experimental situations, when the surfaces are large and adsorbing and the polymers are long. Using a recently presented density functional theory, we are able to compare predictions for chains of finite and infinite length. A major advantage of the infinite chain formulation is that it is a high resolution theory, and predictions from the finite length version will exactly approach the ones for infinite chains, when the degree of polymerization becomes large enough. Our study spans across a relatively large number of relevant system parameters, such as bulk concentration, surface adsorption strength, polymer length, and chain flexibility. The response in terms of the net surface interaction, to a change of a system parameter, is often nonmonotonic. We also make comparisons with predictions at full equilibrium, where the diffusion constraint has been relaxed. We give a specific example of how a diffusion-limited process can lead to hysteresis effects, similar to those observed in many surface force measurements. Finally, in a separate section of this work, we have included some direct experimental comparisons, demonstrating the relevance and applicability of restricted equilibrium conditions to "real world" scenarios. The computational power of the density functional approach is here highlighted, with calculations including semiflexible 20000-mers.

1. Introduction

Polymers are known to have a substantial influence on the interaction between surfaces and particles, sometimes even at long range. This property is used in nature as well as in many industrial processes. Scientists have made considerable efforts to understand and predict how surface forces are affected by the presence of polymers. One major problem is the very large number of parameters that are required to characterize a given system. On the other hand, this is also why polymers find such a wide range of applications. Relevant system parameters, for neutral polymers include the following: chain length; polydispersity; solvent−monomer, monomer−monomer, and solvent−solvent interactions; solvent−surface and monomer−surface interactions; intrinsic chain stiffness; polymer architecture (block, star etc.); temperature; polymer concentration and solution compressibility. Unfortunately, specifying even all of these parameters may still not suffice to characterize the system completely. Nonequilibrium effects are often considerable, and can sometimes dominate the overall behavior. This is obvious from surface force measurements, where the interaction for approaching surfaces commonly differs, even qualitatively, from the one obtained when the surfaces are drawn apart.[1] In a true equilibrium situation they would coincide. It is generally believed that a major contribution to the observed nonequilibrium effects, is a diffusion-limited bulk exchange of polymers, as the surface separation is changed. This suggestion is supported by the fact that equilibrium curves usually are obtained between polymer brushes, where essentially all chains are anchored to the surfaces.[2] Effects due to slow diffusion processes are expected to be particularly relevant when the average degree of polymerization is large.

A common theoretical assumption is that the chains, which have been "captured" between two large surfaces, are still able to equilibrate their configurations. This is is usually defined as "restricted equilibrium".[3−5] This system may be treated with an equilibrium theory, by introducing a semipermeable membrane at the edges of the slit preventing exchange of polymers with the bulk, but allowing free diffusion of solvent particles.

In this work, we will investigate forces between large flat surfaces in the presence of polymers, under the restricted equilibrium constraint below a threshold separation. We will use density functional theory (DFT), including a recently reported version for chains of infinite length.[6] This theory is able to resolve structural details at the monomer length scale, and fulfills thermodynamic sum rules, such as the contact value theorem. This is in contrast to the commonly used Edwards−deGennes theory,[3,7−14] where predictions only can be made at a coarse-grained level. Several additional approximations are usually added to the original Edwards formulation, in order to tailor the theory to various circumstances (small density gradients etc.), and the validity of these assumptions is rarely demonstrated by explicit examples. This is partly due to fundamental difficulties associated with direct comparisons with, for instance, simulations. These problems are not only imposed by the obvious difficulties of simulating "infinite" (very long) polymers, but are also related to the inability of the theory to handle structural details. For instance, the polymer−surface

* Corresponding author. E-mail: jan.forsman@teokem.lu.se.
† E-mail: c.woodward@adfa.edu.au.

10.1021/ma071181t CCC: $37.00
Published on Web 10/19/2007

Hamiltonian is often replaced by physically ambiguous boundary conditions.

Additional approximations to the Edwards theory may lead to erroneous conclusions. For example, deGennes[3] predicted a generally monotonic repulsive surface force in the presence of infinite polymers, under restricted equilibrium conditions at the mean-field level. The analysis contained a number of approximations, and subsequent studies[5,14] have shown that this prediction does not apply to systems where the chains have finite length, even when they are rather long. As we shall see below, it is not supported by a full solution of the mean-field density functional theory either, even for chains of infinite length. Another prediction by deGennes (in the same work) was that surface forces are monotonically attractive under conditions of full equilibrium. This prediction has been confirmed by infinite chain density functional calculations,[6] but sometimes significant free energy barriers are present even for very long chains. In other words, the approach to infinite length behavior is in some cases quite slow. An interesting finding in deGennes' work was that, when the restricted equilibrium case was analyzed at the same level of approximation as the corresponding problem at full equilibrium, a *zero* force prediction was obtained.

Finally, it is worth mentioning the "scaling" approach, introduced by deGennes[3] to treat infinite polymers between surfaces. This approach is not able to resolve structure at the monomer length scale, which may have an important bearing on surface forces, especially with respect to the extent to which this structure governs adsorption onto surfaces. In this work, we shall make comparisons with experimental systems close to Θ conditions, where mean-field theories, such as the density functional theory employed here, are expected to display a reasonable scaling behavior. Furthermore, we also explore athermal systems (effectively good solvents), where the density functional theory has also been shown to provide reasonably accurate predictions, when compared with simulations, at least for relatively short chains.[15,16,31,35]

The density functional formalism can be used to treat flexible as well as semiflexible chains, and it has the added advantage that solvent particles can be easily included *explicitly*, without an incompressibility assumption. In many cases[17−24] an explicit solvent model has uncovered new phenomena. Finally, the density functional theory for infinite chains is a rigorous limit of the theory for finite polymers.[15,16,25] This allows us to properly address the crucial issue about the applicability of infinite chain theory predictions on experimental systems containing polymers of finite length. In other words: how long do polymers need to be in order to be qualitatively regarded as "infinite"? Note that in practice, very long chains find few practical applications, mainly due to problems with diffusion, viscosity and high cost. In our previous work,[6] we found that very high molecular weights are sometimes required to reproduce infinite length behavior, even *qualitatively*. Furthermore, a nonmonotonic dependence of interaction free energy barrier height on the degree of polymerization was found. This is a behavior that cannot be captured by first-order perturbation theories.[26,27] That study was limited to conditions of full equilibrium. In the present case, we perform similar comparisons, but focus on surface interactions under restricted equilibrium conditions.

The density functional formulation is recapitulated in the next section, which is followed by a presentation of our results. These are in turn divided in two separate sections: the first contains detailed theoretical analyses, while the latter focuses on comparisons between density functional predictions and experimental data. The paper concludes with a few summarizing comments.

2. Model and Theory

2.1. Confining Surfaces. We calculate interactions between infinitely large, flat and parallel surfaces. The confining hard walls are perpendicular to the *z*-direction, and are located at $z = 0$ and $z = h$. In addition to the hard, confining interaction, the monomers will in general also sense a surface attraction, $V_{ex}(z, h)$, where

$$V_{ex}(z, h) = w(z) + w(h - z) \tag{1}$$

The first part of our work focuses on purely theoretical analyses, which are simplified by the use of a truncated adsorption potential. Here, we will adopt a Morse potential

$$\beta w_{ex}^{ref}(z) = A([1 - e^{-2(z-z_m)/\sigma}]^2 - 1) \tag{2}$$

where β is the inverse thermal energy, while σ is the monomer diameter. Hence, the "well depth" is directly given by the amplitude factor, *A*. The range of the adsorption potential is limited by a truncation and shift procedure, i.e.:

$$w_{ex}(z) = w_{ex}^{ref}(z) - w_{ex}^{ref}(z_c) \tag{3}$$

The position of the minimum value of the potential, z_m, is defined such that $w_{ex}(z = 0) = 0$. Choosing $z_c - z_m = 2.9$, we obtain $z_m \approx 0.346$. This means that the adsorption potential has no repulsive part (hard walls are located at $z = 0$ and $z = h$, though). Overlap between opposing potentials occurs below separations of about $h = 6.5\sigma$.

In the second part of our work, we shall make comparisons with a specific experimental system, in which dispersion interactions are expected to dominate. Hence, we will in this case adopt an integrated Lennard-Jones adsorption potential:

$$\beta w_{L-J}(z) = 2\pi A_{L-J}\left[\frac{2}{45}\left(\frac{\sigma}{z}\right)^9 - \frac{1}{3}\left(\frac{\sigma}{z}\right)^3\right] \tag{4}$$

where the surface affinity is modulated by the amplitude factor A_{L-J}.

2.2. Finite Chains. Our theory is based Woodward's density functional formalism,[15] but we will adopt further developed versions for flexible[16] and semiflexible[25] polymers. Quite recently,[6] these were generalized to handle the infinite length limit. We first recapitulate the description for finite chains. We denote the position of the *i*th monomer in a chain by $\mathbf{r}_i$. The complete polymer configuration of an *r*-mer can then be written as: $\mathbf{R} = (\mathbf{r}_1, ..., \mathbf{r}_r)$. Neighboring monomers along a chain are connected by bond of a fixed length σ, which also defines their diameter. Hence, $e^{-\beta V_B(\mathbf{R})} \propto \prod_r^{i=1} -1\ \delta(|\mathbf{r}_{i+1} - \mathbf{r}_i| - \sigma)$, where $V_B(\mathbf{R})$ is the bond potential. The density distribution, $N(\mathbf{R})$ is defined such that $N(\mathbf{R})\ d\mathbf{R}$ is the number of polymer molecules having configurations between $\mathbf{R}$ and $\mathbf{R} + d\mathbf{R}$. We can then extract the monomer density $n(\mathbf{r})$ from $n(\mathbf{r}) = \int \Sigma_{i=1}^{r} \delta(\mathbf{r} - \mathbf{r}_i)$-$N(\mathbf{R})\ d\mathbf{R}$. The free energy functional, $F[N(\mathbf{R})]$, contains an ideal ($F^{id}[N(\mathbf{R})]$) and an excess ($F^{ex}[N(\mathbf{R})]$) part:

$$F[N(\mathbf{R})] = F^{id}[N(\mathbf{R})] + F^{ex}[N(\mathbf{R})] \tag{5}$$

The ideal term is given by

$$\beta F^{id}[N(\mathbf{R})] = \int N(\mathbf{R})(\ln[N(\mathbf{R})] - 1)\, d\mathbf{R} + \beta \int N(\mathbf{R})(V_B(\mathbf{R}) + V_{ex}(\mathbf{R}))\, d\mathbf{R} \tag{6}$$

where $V_{ex}(\mathbf{R})$ is the previously defined surface potential. Note that for purely ideal chains, the theory is exact. The excess part has to be approximated. Following Woodward,[15] we formulate it in terms of the monomer density: $F^{ex}[n(\mathbf{r}); \bar{n}(\mathbf{r})]$, where $\bar{n}(\mathbf{r})$ is a weighted density:[28]

$$\bar{n}_m(\mathbf{r}) = \frac{3}{4\pi\sigma^3}\int_{|\mathbf{r}-\mathbf{r}'|<\sigma} n_m(\mathbf{r}')\,d\mathbf{r}' \tag{7}$$

We estimate $F^{ex}[n(\mathbf{r});\bar{n}(\mathbf{r})]$ from an integration of the "Generalized Flory-Dimer" (GFD) equation of state.[29] Explicit expressions are provided in ref 16. Other weight functions and functionals have been suggested and compared,[30,31] but the specific choice is less relevant to this study, which focuses on solutions with an implicit solvent and a low monomer concentration.[31]

The grand potential, Ω, is obtained from

$$\Omega[N(\mathbf{R})] = F^{id}[N(\mathbf{R})] + F^{ex}[n(\mathbf{r});\bar{n}(\mathbf{r})] - \mu_p\int N(\mathbf{R})\,d\mathbf{R} \tag{8}$$

where μ_p is the chemical potential of the polymer fluid in the bulk. By minimizing the grand potential we obtain the corresponding equilibrium density distribution, $N_{eq}(\mathbf{R})$. However, in our model system, bulk exchange is prevented below a threshold surface separation h_T. Above this separation, we relax the constraint and assume full equilibrium. This serves as an idealized model of the diffusion-limited processes discussed in the previous section. It should be emphasized that we, unless otherwise specifically stated, allow for complete adsorption equilibrium at h_T. The theoretical part of this work only consider such situations. When we proceed to make comparisons with experiments, we will also investigate the interesting and relevant scenario of undersaturated surfaces (incomplete incubation time).

At separations below h_T, the diffusion constraint is conveniently handled by a potential, $\Phi(h)$, which adjusts with separation so as to conserve the number of monomers in the slit. $\Phi(h)$ acts uniformly across the slit, and serves a similar purpose as the Donnan potential in electrolyte theory, where it enters to ensure electroneutrality. Specifically, we obtain the following expression for the density distribution:

$$N_{eq}(\mathbf{R}) = e^{\beta(\mu_p - V_B(R))}\prod_{i=1}^{r} e^{\Phi(h)-\beta\lambda(\mathbf{r}_i)} \tag{9}$$

where

$$\lambda(\mathbf{r}) = \beta(\delta F_{ex}/\delta n(\mathbf{r}) + V_{ex}(\mathbf{r})) \tag{10}$$

We emphasize that $\Phi(h > h_T) = 0$, and that this potential is a mathematical way to treat the way in which diffusion restriction modulates our reference "full equilibrium functional". This allows us to prevent bulk exchange and yet retain the functional form, eq 8.

The free energy per unit area, $g(h)$, is given by $g(h) = \Omega_{eq}/S + P_b h$ where Ω_{eq} is the equilibrium grand potential and P_b is the osmotic pressure in the bulk. The symmetry, coupled with our mean-field assumption, allows us to integrate away all (x, y) dependence. At large separations, g approaches twice the tension at a single surface, γ_s. However, since our focus is on restricted equilibrium conditions, we have in most cases used the definition $\Delta g(h) \equiv g(h) - g(h_T)$; i.e., we measure free energies relative to a reference at the transition distance.

The intrinsic rigidity of semiflexible polymers is modeled via a stiffness potential, E_B, which effectively imposes a repulsion between next nearest neighbors in a chain. If we by $\mathbf{s}_i$ denote the bond vector between monomers i and $i+1$, we can write E_B as follows: $\beta E_B = \epsilon(1 - (\mathbf{s}_i\cdot\mathbf{s}_{i+1})/\sigma^2)$, where ϵ regulates the strength of the stiffness potential. Furthermore, with $\Delta z_i \equiv z_{i+1} - z_i$, we can write the vector product as

$$\mathbf{s}_i\cdot\mathbf{s}_{i+1} = \Delta z_i\Delta z_{i+1} + (\sigma^2 - \Delta z_i^2)^{1/2}\times (\sigma^2 - \Delta z_{i+1}^2)^{1/2}\cos\phi_{i,i+1} \tag{11}$$

where $\phi_{i,i+1}$ is the angle between $\mathbf{s}_i$ and $\mathbf{s}_{i+1}$, as projected onto the plane of the surfaces. If we average the Boltzmann factor over the surface plane, we get the following:

$$\Psi(\Delta z_i, \Delta z_{i+1}) = e^{-\epsilon(1-(\Delta z_i\Delta z_{i+1})/\sigma^2)} I_0 \times \left[\epsilon\left(1-\left(\frac{\Delta z_i}{\sigma}\right)^2\right)^{1/2}\left(1-\left(\frac{\Delta z_{i+1}}{\sigma}\right)^2\right)^{1/2}\right] \tag{12}$$

Here $I_0(x) = (1/2\pi)\int_0^{2\pi}\exp[-x\cos\phi]\,d\phi$ is a modified Bessel function, which can be evaluated from a polynomial expansion. The equilibrium monomer density profile, which minimizes the free energy, reads as follows:

$$n(z) = e^{\beta\mu_p}\sum_{i=1}^{r}\int_0^h \delta(z-z_i)\sum_{j=1}^{r} e^{-\lambda(z_j)}\sum_{k=1}^{r-1}\Theta(|\Delta z_k| - \sigma)\sum_{l=1}^{r-2}\Psi(\Delta z_l, \Delta z_{l+1})\,dz_1\ldots dz_r \tag{13}$$

Here $\Theta(x)$ is the Heaviside step function,

$$\Theta(x) = \begin{cases} 1 & , x \le 0 \\ 0 & , x > 0 \end{cases} \tag{14}$$

The notation is simplified by the omission of the special treatment of end monomers in the GFD functional[16] (they were handled appropriately in the calculations, though). By neglecting effects from hard core repulsions, we can estimate several relevant single chain properties. For instance, denoting the position vector between end monomers by $\mathbf{R}_{ee}$, we can evaluate the persistence length, $\xi_p = \langle\mathbf{R}_{ee}\mathbf{s}_1/\sigma\rangle$, as

$$\xi_p/\sigma = \frac{\epsilon(1-e^{-2\epsilon})}{1-e^{-2\epsilon}(1+2\epsilon)} \tag{15}$$

Even for moderate values of ϵ, this simplifies to $\xi_p/\sigma \approx \epsilon$, which perhaps provides a more intuitive interpretation of the stiffness parameter. Furthermore, the root-mean-square end-to-end separation, $R_e \equiv \langle\mathbf{R}_{ee}\mathbf{R}_{ee}\rangle^{1/2}$, is given by

$$\frac{\langle\mathbf{R}_{ee}\mathbf{R}_{ee}\rangle}{\sigma^2} = r - 1 + 2\sum_{i=1}^{r-2}(r-1-i)\left[\frac{e^{-2\epsilon}(1+\epsilon)+\epsilon-1}{\epsilon(1-e^{-2\epsilon})}\right]^i \tag{16}$$

where the brackets, $\langle\ldots\rangle_\epsilon$ denote a Boltzmann weighted orientational average, at the given stiffness parameter, ϵ.

We first describe how eq 13 can be solved for the simpler case of flexible ($\epsilon = 0$) polymers, in which case the last product is unity. We define an auxiliary field $c_f(i,z)$, for position i along the chain. Equation 13 can then, for flexible chains, be written as:[6,30,32]

$$n(z) = \rho_p^b\sum_{i=1}^{r} c_f(i,z)c_f(r+1-i,z) \tag{17}$$

where ρ_p^b is the bulk polymer density. $c_f(i,z)$ fulfills a recursive relation (for $2 \leq i \leq r$):

$$c_f(i,z) = e^{\lambda_b} \int c_f(i-1,z')T(z',z)\,dz' \quad (18)$$

with $c_f(1,z) = 1$. Here, λ_b is the value of λ in the bulk, which one may refer to as the "excess monomer chemical potential". The connectivity matrix, $T(z,z')$, is defined as

$$T(z',z) = \frac{e^{-\lambda(z')/2}\Theta(|z-z'|-\sigma)e^{-\lambda(z)/2}}{2\sigma} \quad (19)$$

With semiflexible chains, the corresponding solution requires a three-dimensional matrix, $c_s(i,z,z')$, which should be used sparsely if computational efficiency is of interest, i.e., for long chains (see below). The connectivity matrix, $T_s(z,z')$, now reads:

$$T_s(z',z) = \frac{e^{-\lambda(z')/3}\Theta(|z-z'|-\sigma)e^{-\lambda(z)/3}}{2\sigma} \quad (20)$$

The monomer density is obtained from

$$n(z) = \rho_p^b \sum_{i=1}^{r} \int c_s(i,z,z'-z)c_s(r+1-i,z',z-z')T_s(z,z')\,dz' \quad (21)$$

with the following closure:

$$c_s(i,z,z'-z) = e^{2\lambda_b/3} \int c_s(i-1,z'',z-z'') \times \Psi(z-z'',z'-z)T_s(z,z'')\,dz'' \quad (22)$$

2.3. Infinitely Long Chains. In an infinitely long polymer, all monomers are equivalent, i.e., all monomers are "central". It may be useful to think of it as a very large ring polymer. The equivalence of all monomers simplifies the iterative procedure considerably, which now can be formulated as

$$n(z) = n_b \gamma_f^2(z) \quad (23)$$

where n_b is the monomer density in the bulk solution. The vector $\gamma_f(z)$ fulfills the closure

$$\gamma_f(z) = e^{\lambda_b} \int \gamma_f(z')T(z',z)\,dz' \quad (24)$$

These equations are rapidly solved in an iterative manner.

With semiflexible chains, the corresponding solution requires a two-dimensional matrix, $\gamma_s(z,z')$, but the iterative relations are still simple:

$$n(z) = n_b \int \gamma_s(z,z'-z)\gamma_s(z',z-z')T_s(z,z')\,dz' \quad (25)$$

with

$$\gamma_s(z,z'-z) = e^{2\lambda_b/3} \int \gamma_s(z'',z-z'')\Psi(z-z'',z'-z) \times T_s(z,z'')\,dz'' \quad (26)$$

The formalism above (for finite and infinite chains) is general in the sense that it does not rely on any specific choice of the approximate part, F_{ex}. We shall primarily be using a GFD functional, the high accuracy of which has been demonstrated in several studies.[16,29,33−36] There are in principle other viable options,[37−40] which display an accuracy comparable to the GFD. They would be likely to produce results similar to those found in this work.

As we pointed out in our previous study,[6] an interesting alternative would be to use a continuum DFT version[41] of the Scheutjens−Fleer theory.[42] An important point is that this kind of theory relies on a different view of the solutions, since the solution is assumed to be completely incompressible, even on a local scale. We will therefore include a comparison with predictions from such a model at the very end of this work. With this exception, we will use the GFD functional as described above, and thus implicitly assume that solvent effects are captured via the monomer−monomer potential of mean force and McMillan−Mayer theory.

2.4. Computational Efficiency. In the second part of our work, we will compare DFT predictions on flexible and semiflexible polymer models, with experimental surface force data. These comparisons are in general made for very long chains, up to 20000-mers. In those cases, it is worthwhile to make some effort to optimize the computational efficiency of the code, in particular for the semiflexible chains. Below we list a few useful strategies:

•Higher order vectors are used as seldom as possible. For example, integrals, such as eq 18 are more rapidly evaluated if we introduce "alternating vectors" cA(z) and cB(z). If we define

$$cB(z) = e^{\lambda_b} \int cA(z')T(z',z)\,dz' \quad (27)$$

followed by an updating loop which sets $c(i,z) = cB(z)$, we can set

$$cA(z) = e^{\lambda_b} \int cB(z')T(z',z)\,dz' \quad (28)$$

and $c(i+1,z) = cA(z)$ and so on. Evaluating integrals with lower order vectors is even more important for semiflexible chains, in which case we replace the three-dimensional vector $c(i,z,z-z')$ by two-dimensional "alternating vectors" $cA(z,z-z')$ and $cB(z,z-z')$. For long chains this trick speeds up the code considerably.

•Good initial guesses for the iterative solutions are made. For the first calculation, one might use the corresponding infinite chain predictions. The latter are obtained (somewhat paradoxically) very quickly. Once a solution at one separation is obtained, it can be suitably scaled to provide an initial guess for a density at another surface separation.

•The DFT parallelizes extremely well. We have only tested up to four processors, for which we get a speed-up of 4.0

•Matrices are indexed in an optimal fashion. This depends on the language in which the program is written (e.g., Fortran or C) as well as the nature of the solution algorithm itself.

3. Results

Only monodisperse polymer solutions are considered. In order to estimate the thermodynamic significance of the calculated interactions, we will sometimes compare our results with the nonretarded van der Waals ("vdW") attraction, using a typical Hamaker constant of 10^{-20} J.

3.1. Theoretical Analysis. In this section, we only consider athermal hard core polymer fluids ("good solvent conditions"), and the surfaces are of the "truncated Morse potential" type, eq 3.

We will investigate how the polymer mediated surface interactions respond to changing the following system parameters:

•chain length, r;

•surface affinity, A;

•intrinsic chain stiffness, ϵ;

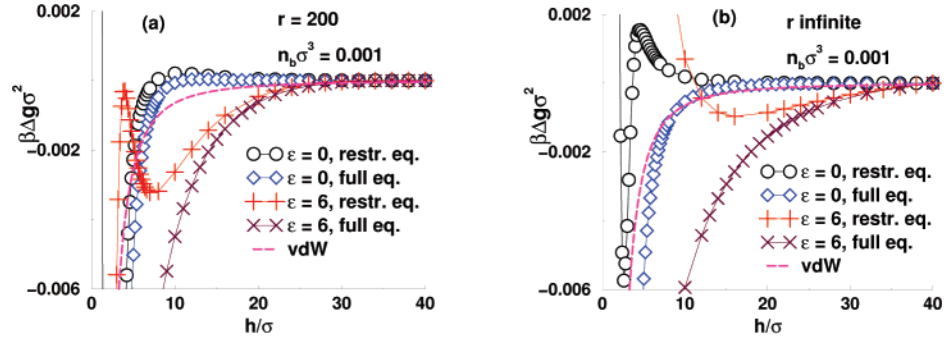

Figure 1. Comparison between surface interaction free energies at full and restricted ($h_T = 40\sigma$) equilibrium, respectively. The surfaces are adsorbing ($A = 1$) and the bulk monomer concentration is $n_b\sigma^3 = 0.001$. The dashed line shows a nonretarded van der Waals (vdW) attraction, assuming a Hamaker constant of $1E - 20$ J. Surface forces at full and restricted equilibrium are given for all four reference systems. (a) Solutions containing flexible ($\epsilon = 0$) and semiflexible ($\epsilon = 6$) 200-mers. (b) Solutions containing flexible ($\epsilon = 0$) and semiflexible ($\epsilon = 6$) infinitely long chains.

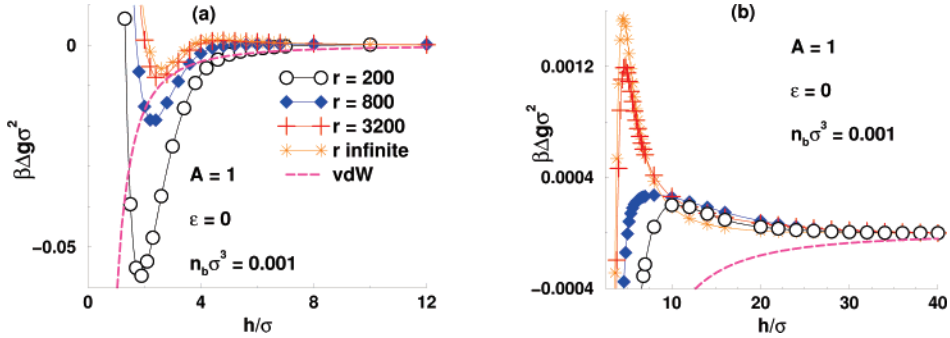

Figure 2. Interaction free energies between adsorbing surfaces, at restricted equilibrium conditions ($h_T = 40\sigma$), in solutions containing flexible polymers. Each curve represents a monodisperse solution, where all chains have a given length r. Note that $\Delta g(h) \equiv g(h) - g(h_T)$. The dashed line is as defined in Figure 1. Graph b is a blow-up of the repulsive regime at long range.

•bulk monomer concentration, n_b.

In particular, we consider varying these quantities around the following "reference" values: $r = 200$; $A = 1$; $\epsilon = 0$ or 6; $n_b\sigma^3 = 0.001$. Unless otherwise stated, restricted equilibrium conditions will apply at separations below $h_T = 40\sigma$. In the next section (containing experimental comparisons) we shall adopt a larger value of h_T. We will also investigate effects of how diffusion limitation can generate hysteresis effects.

3.1.1. Full vs Restricted Equilibrium. We have performed calculations for polymer solutions with both full and restricted equilibrium boundary conditions. In Figure 1a, we consider the reference systems. Note that the free energy is only shown for $h < h_T$. For the restricted equilibrium case

$$\frac{d\Delta g(h)}{dh} = \beta^{-1}n(h) - \int_0^h n(z)\frac{\delta V_{ex}(z,h)}{\delta h}dz + P_b + \Phi(h)\int_0^h \frac{\delta n(z)}{\delta h}dz \quad (29)$$

where P_b is the bulk pressure, and the last term is zero at all separations, as $\Phi(h) = 0$ for separations above h_T, and the monomer surface density is conserved for separations below h_t. $n(h)$ is the monomer density adjacent to the surface, and is a continuous function of h. Thus, $\Delta g(h)$ is continuously differentiable at $h = h_T$ for both full and restricted equilibrium boundary conditions. Figure 1a clearly shows that systems with restricted equilibrium generally display less attractive interactions when compared with the completely relaxed case. The degree of difference between these systems depends upon the polymer length and the intrinsic chain stiffness. In particular, we note how the restricted equilibrium curve deviates strongly from the relaxed one even at relatively large separations, in the presence of semiflexible chains ($\epsilon = 6$) of infinite length, Figure 1b. The occurrence of a short-ranged attraction ($h < 5\sigma$), sometimes accompanied by a free energy barrier in some systems may be due to either polymer bridging or the interaction of the potential well from one surface with polymers adsorbed on the other surface. As will be discussed later, both these attractive mechanisms may become important at short-range, especially for flexible polymers. Remember that adsorption potentials on opposing surfaces start to overlap below $h \approx 6.5\sigma$. On the other hand, for semiflexible polymers, attractions at longer range ($h > 10\sigma$) is unambiguously due to polymer bridging.

3.1.2. Chain Length. In Parts a and b of Figure 2, we investigate the role played by the degree of polymerization, r, for fully flexible chains. We see that, in all the cases we studied, there is a barrier at $h \approx 5\sigma$, with an attractive well at shorter separations. The depth of the well, and the barrier height, depend strongly on the length of the dissolved polymers. For example, we note that the well-depth is dramatically reduced as the molecular weight increases. Figure 2b focuses on the repulsive regime at long range. Here, we see that shorter chains generate a stronger repulsion at long range, presumably due to the presence of more tails. However, the height of the free energy barrier increases with r, thus the free energy curves cross each other. As mentioned above, this barrier is due to the structure of adsorbed monomers. The amount adsorbed is greater for larger r, due to greater cooperativity.

The corresponding interactions for semiflexible chains ($\epsilon = 6$) are qualitatively different from the flexible case, with an attraction at long range that increases with polymer length. This is illustrated in Figure 3. This attraction is generated by strong bridging interactions (as will be discussed later) and is considerably stronger than the expected van der Waals interaction at these separations. In the presence of 200-mers, there is a free energy barrier, and a strong attraction at short range. This

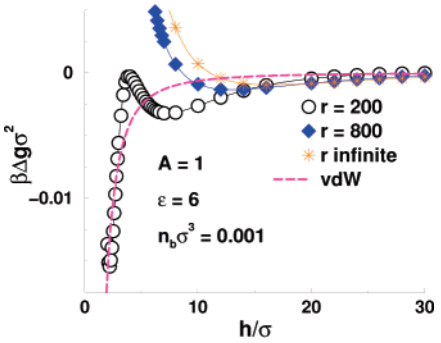

Figure 3. Surface interactions under the same conditions and in Figure 2, but where the chains are semiflexible: $\epsilon = 6$. The dashed line is as defined in Figure 1.

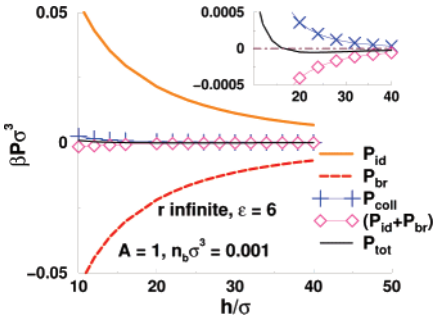

Figure 4. Separate contributions to the osmotic pressure acting across the mid plane of the slit, for the infinite chain length system displayed in Figure 3. The inset is a blow-up where the sum of the ideal (P_{id}) and bridging (P_{br}) contributions can be more carefully compared with the collisional term, P_{coll}. P_{tot} is the total internal osmotic pressure in the slit, acting perpendicular to the surfaces. Note that we only display the long range part, where there are no monomer−surface interactions across the mid plane, i.e., $P_{surf} = 0$. At infinite surface separation, $P_{id} + P_{br} = 0$, while $P_{coll} = P_b$. In the present case, the bulk pressure is small, $\beta P_b \sigma^3 < 10^{-6}$.

is absent for the systems with the higher degree of polymerization. This is because the average monomer density in the slit is greater for longer polymers. The resulting entropic confinement of the longer chains leads to a larger repulsive free energy contribution, which dominates the surface interaction at shorter separations.

An important advantage of a high resolution theory of the kind considered here, is that it is possible to scrutinize the interactions in a mechanistic fashion, by extracting the separate contributions to the total osmotic pressure acting across the midplane (perpendicular to the surfaces). In an athermal system, these contributions are as follows:

- a repulsive ideal entropic pressure, P_{id}, simply given by the total monomer density at the midplane;
- a repulsive collisional pressure, P_{coll}, caused by hard core interactions between monomers on either side of the midplane;
- an attractive pressure, P_{surf}, from particles on one-half of the midplane interacting with the surface on the other side;
- an attractive bridging term, P_{br}, from intrachain bonds crossing the midplane.

Explicit expressions for these has been presented elsewhere.[43,44] Furthermore, the total internal osmotic pressure is given by: $P_{tot} = P_{br} + P_{id} + P_{coll} + P_{surf}$, which approaches the bulk pressure, P_b, at large separations. Although P_{coll} is termed a "collisional" contribution, it should be noted that its origin actually stems from configurational constraints imposed by the excluded volume of particles, and not from impulsive forces.

The dependence of these components on the separation, h, for infinite semiflexible polymers is given in Figure 4. Clearly, P_{id} and P_{br} dominate the surface interaction at these separations, but since the degree of polymerization is infinite, these components will exactly cancel as the surfaces are drawn far apart. Specifically, $-\beta P_{br} = \beta P_{id} = n_b$, at infinite separation. Thus, we have also plotted their sum, which is more clearly depicted in the inset of Figure 4. The attractive regime of the surface pressure occurs where P_{coll} is larger than its bulk value, P_b. Hence, the attraction is due to the bridging component, which dominates the sum, $P_{id} + P_{br}$.

3.1.3. Surface Affinity. The polymer mediated interaction between two surfaces will also depend strongly on the monomer−surface interaction. This is clearly demonstrated in Figure 5, for flexible chains. For 200-mers, Figure 5a, there is a nonmonotonic response, as the surface potential strength, A, is increased. At $A = 0$, the surface interaction is repulsive. This is due to the reduction in configurational and conformational entropy of the confined chains as the surfaces approach. Here, it should be pointed out that, in practice, one would not expect restricted equilibrium conditions to prevail when the surfaces are nonadsorbing. Still, $A = 0$ serves as a useful reference, i.e., the asymptote of very weak adsorption. Increasing to $A = 1$ leads to the appearance of an attractive well, as seen before. However, for $A = 2.5$, there is a counterintuitive decrease of the well-depth. This is due to the increased number of monomers drawn into the interstitial region at $h = h_T$, when A is increased. A similar effect was seen above when we considered the r dependence of the interaction. Qualitatively similar behavior is demonstrated for infinitely long polymers, Figure 5b. Note, however, that the free energy minimum that occurs at $A = 1$ is about an order of magnitude deeper with the shorter chains. Furthermore, in the presence of infinitely long chains, the surface force appears, on this scale, to be monotonically repulsive at $A = 2.5$.

The inset of Figure 5b highlights the transition between full and restricted equilibrium at $h = h_T$ for infinite chains. In agreement with a theorem by deGennes,[3] the fully equilibrated system is attractive at large h. Furthermore, as pointed out earlier, the interaction free energy is continuously differentiable at h_T. Thus, in this region the interaction between surfaces at restricted equilibrium will be attractive, albeit weakly so. This fact is fundamentally interesting, because the attraction at h_T follows from the deGenne's theorem for fully equilibrated systems, which has been confirmed (at least numerically) by density functional calculations of the kind adopted in this study.[6] This suggests that the attraction may well be a ubiquitous phenomenon for restricted equilibrium systems with the type of sample history described here.

In parts a and b of Figure 6, we investigate the role played by surface potential strength for semiflexible polymers ($\epsilon = 6$). For 200-mers, we once again find a nonmonotonic response to increasing A. For purely hard walls the interaction free energy is repulsive, except very close to h_T. For moderately attractive surfaces ($A = 1$), a strong attraction persists down to small distances. However, a repulsive free energy is reestablished at large separations for $A = 2.5$, together with an attractive well at smaller separations. With adsorbing surfaces, the attractive regimes are due to strong bridging interactions. As with flexible polymers the nonmonotonic behavior with respect to the adsorption strength is due to increasing number of monomers per unit area, which increases the repulsive P_{id} and P_{coll} components to the osmotic pressure.

For infinite polymers, however, there is a monotonic response to the adsorption potential strength, as shown in Figure 6b. With

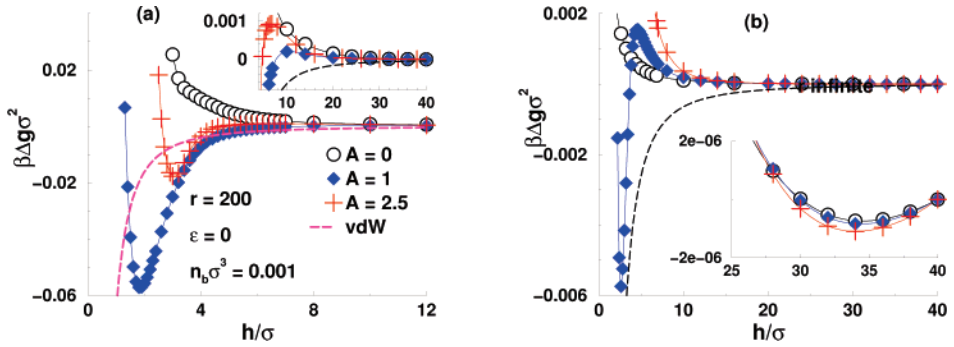

Figure 5. Surface force dependence on adsorption potential potential strength, A, in the presence of flexible chains. Restricted equilibrium conditions ($h_T = 40\sigma$). The dashed line is as defined in Figure 1. (a) 200-mers. The inset is an enlargement of wide slit widths. (b) Infinite degree of polymerization. The inset is a blow-up, demonstrating the existence of a weak attraction at very long range, close to h_T.

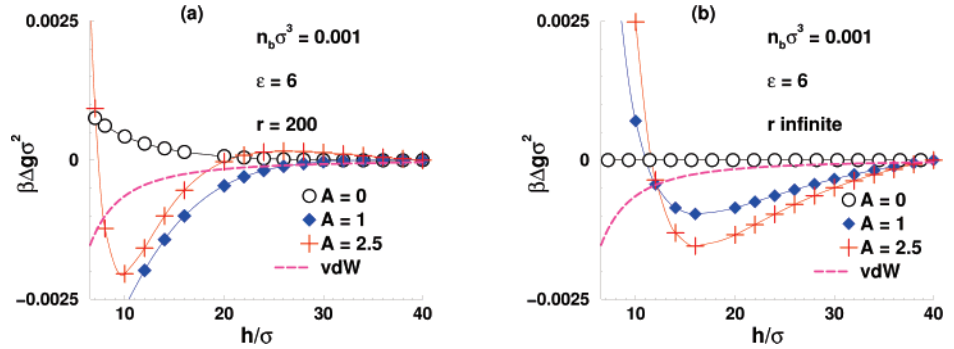

Figure 6. Responses to changes of the surface affinity, in the presence of semiflexible chains, $\epsilon = 6$. Restricted equilibrium conditions apply below $h_T = 40\sigma$ The dashed line is as in Figure 1. Key: (a) 200-mers; (b) infinite degree of polymerization.

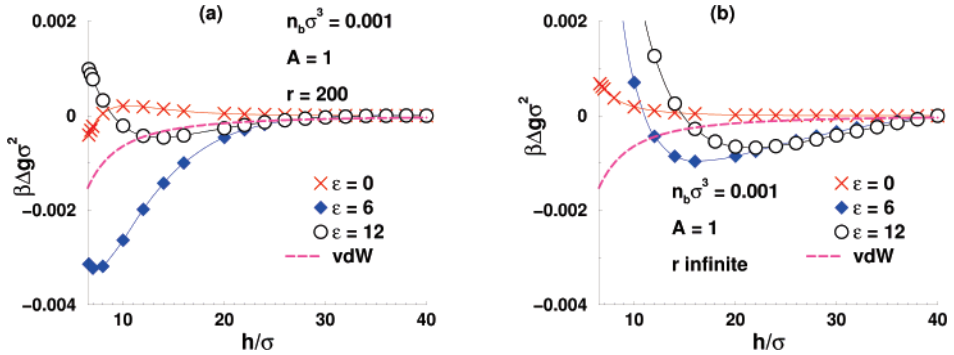

Figure 7. Effects of intrinsic chain stiffness, as regulated by the parameter ϵ, under restricted equilibrium conditions ($h_T = 40\sigma$). The dashed line is as defined in Figure 1. Key: (a) $r = 200$; (b) r infinite.

purely hard walls, $A = 0$, the slit is depleted of monomers for $h \leq h_T$. Hence, Δg is zero in this regime. Increasing the surface attraction leads to progressively deeper attractive wells occurring at around $h = 15\sigma$. This attraction is due to bridging interactions. We see in general that the depth of the attractive well is weaker, but more long-ranged, than in the finite-sized polymer systems ($r = 200$). This is due to the higher monomer density between the surfaces for infinite chains, which increases the repulsive osmotic pressure components. On the other hand, the interaction free energy at long range is less attractive for finite chains. This is due to overlap of tails of adsorbed polymers, which add to repulsive forces but contribute weakly to bridging.

3.1.4. Intrinsic Chain Stiffness. In Figure 7, we compare the interaction between surfaces, immersed in solutions with the same bulk density, but where the intrinsic chain rigidity is different. Again, it appears that the for finite sized polymers ($r = 200$), the response is nonmonotonic. While fully flexible chains induce a free energy barrier, moderately stiff ones ($\epsilon = 6$) generate a strong and rather long-ranged attraction. With a further increased stiffness ($\epsilon = 12$), this attraction becomes considerably weaker, turning repulsive already at $h \approx 10\sigma$. This response is qualitatively similar when the chain length is infinite, but in this case the stiffest chains generate an attractive well that is almost as deep as with the moderately stiff ones. At long range, the attraction is even slightly stronger.

3.1.5. Bulk Monomer Concentration. One would expect that under conditions of restricted equilibrium, i.e., below h_T, the surface interactions become more repulsive at higher bulk monomer concentrations (assuming full equilibrium at h_T). This is because the fixed internal monomer surface density, determined at $h = h_T$, becomes larger as n_b increases. This conjecture is confirmed by the results shown in Figure 8. Indeed, for flexible, infinite polymers, reducing the bulk monomer concentration by an order of magnitude ($n_b\sigma^3 = 0.0001$) gives rise to a monotonically attractive surface interaction. This is qualitatively different to the repulsive interactions seen at the higher densities, $n_b\sigma^3 = 0.001$, 0.01. Indeed, for $n_b\sigma^3 = 0.01$, the onset of the repulsive interaction occurs at quite large separation. Clearly there is an interplay between repulsive entropic and collisional interactions and attractive bridging

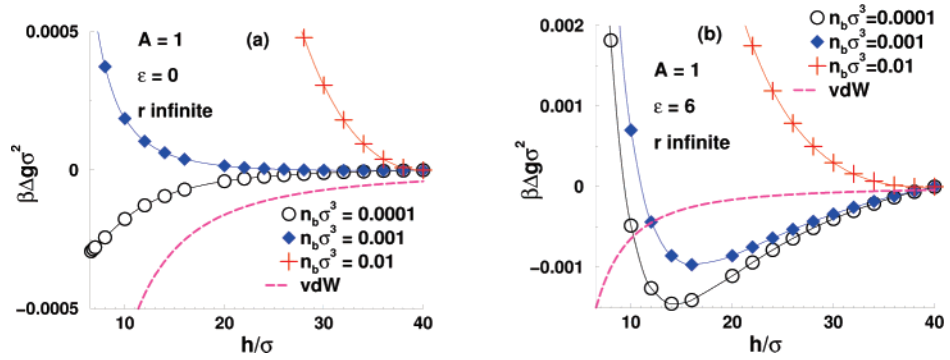

Figure 8. Restricted equilibrium ($h_T = 40\sigma$) interactions between surfaces immersed in solutions containing infinitely long chains, at various bulk monomer concentrations. The dashed line is as defined in Figure 1. Key: (a) fully flexible chains, $\epsilon = 0$; (b) semiflexible chains, $\epsilon = 6$.

interactions, as the monomer density is changed. At low concentrations, the bridging component dominates, leading to an overall attractive interaction, while at higher density the repulsive terms are larger. One can qualitatively understand these effects by realizing that the entropic and bridging terms would scale approximately linearly with the monomer density, while the collisional term is expected to have a higher order (at least quadratic) density dependence.

One might argue that the concept of restricted equilibrium, at least in the sense we have defined it, is less likely to be a valid description of an experimental scenario when the monomer concentration is high. This is because at high concentrations the adsorbing surfaces tend to become fully saturated, and the slit may contain quite a few chains that are essentially unadsorbed ("expelled"). Those chains are likely to follow the solvent as it exchanges with the bulk when the separation is changed.

Similar behavior is observed for semiflexible polymers, except that the attractive interactions, obtained for the dilute cases, extend to larger separations. This is expected, given the longer range of the bridging interactions. Furthermore, at shorter separations ($h < 10\sigma$), the interactions turn repulsive, due to the compression of stiffer chains. Large effects of intrinsic chain rigidity on surface interactions, have also been found at full equilibrium conditions.[6,36,44]

Finally, it should be remarked that the surface force is less sensitive to changes to the monomer density when the concentration is low. This will be highlighted in the "Experimental comparisons" section.

3.1.6. Nonequilibrium Hysteresis Effects. As already mentioned, experimental surface force measurements in polymer solutions frequently display hysteresis effects, indicative of inhibited diffusion (nonequilibrium) processes. Specifically, the measured surface interactions on approach usually differ considerably from those when the surfaces are drawn apart. In Figure 9, we have illustrated how this can occur, according to the model described above. The thin solid line describes the "usual case", where restricted equilibrium is imposed at $h_T = 40\sigma$, as the surfaces are pushed together. With infinite, fully flexible chains, this leads to a repulsion. We assume that the surfaces are pushed together to a distance of $h = 5\sigma$, and kept there for a time long enough to permit the establishment of complete equilibrium with the bulk solution. As the surfaces are drawn apart, no further exchange with the bulk is allowed. The corresponding surface interaction is given by the thick solid line. In this case, we find a strongly attractive interaction, in qualitative agreement with most surface force experiments. The plateau value for the free energy is higher than for the interaction free energy on approach. This is expected, given the system is

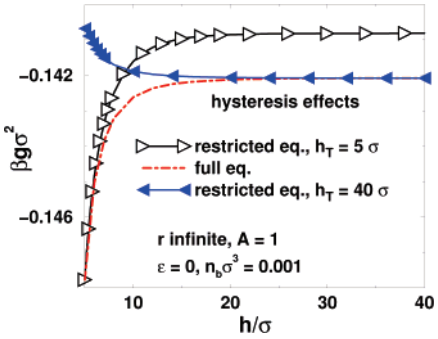

Figure 9. Example of a possible hysteresis effect, caused by diffusion-limited processes. The surfaces are adsorbing ($A = 1$) and the chains are infinitely long, and fully flexible. Triangles pointing left describe the interaction as the surfaces are pushed together, imposing diffusion restricted equilibrium at $h_T = 40\sigma$. Imagine that the surfaces then are allowed to relax completely, including bulk exchange, at $h = 5\sigma$. Triangles pointing right are results obtained if the surfaces subsequently are pulled apart, again under the assumption of restricted equilibrium, but in this case with $h_T = 5\sigma$. The dot-dashed line is a reference, describing the surface interaction at complete equilibrium. Notice that the *total* free energy per unit area (g) is displayed; i.e., we do not subtract the value at some given separation.

kept in a nonequilibrium state. In an actual experiment, one would expect the reestablishment of bulk exchange at large surface separations.

3.2. Experimental Comparisons. In this section, we will make comparisons between density functional predictions and some available experimental data. The Derjaguin approximation is used in order to relate the interaction free energy per unit area in our planar system, to the force per radius of curvature, F/R, measured in the experiments.

Thus far our model has assumed athermal conditions for the polymer solution; i.e., monomers interact as hard cores giving rise to temperature independent behavior in the bulk. This corresponds to a Flory−Huggins interaction parameter $\chi = 0$, a good solvent. However, it is difficult to match these conditions experimentally, as we usually have little knowledge of the monomer−monomer potential of mean force. Another drawback with good solvent conditions is that measured surface forces generally display considerable hysteresis effects, which makes it difficult to unambiguously establish the data with which the DFT predictions should be compared. On the other hand, Θ conditions are generally better determined, as the temperature at which the effective second virial coefficient is zero. In addition, mean-field theories (like our DFT) are more applicable to Θ conditions, where intrachain correlations cancel out, leading to ideal-chain configurational behavior. Thus, we shall primarily make comparisons with experiments performed at or near Θ conditions.

There have been several previous attempts to theoretically describe interactions between adsorbing surfaces in a homopolymer solution. Apart from the Scheutjens−Fleer mean-field SCF approach,[5] Pincus, Klein, and co-workers[11,12,45,46] have developed and used deGennes[3] simplified density functional description of polymer adsorption. In cases where quantitative comparisons with experimental data have been made, the range and strength of the interactions has generally been underestimated under Θ conditions. Still, Klein and Rossi[46] did find good agreement with experimental data at close separations in a *good* solvent.

3.2.1. Polymer Solution Models. In our comparisons, we choose to focus on a surface force apparatus study by Almog and Klein (AK),[47] of interactions between mica surfaces in a polystyrene−cyclopentane solution near the Θ temperature. We will also compare with other experiments, under Θ conditions, where the mica surfaces were immersed in polystyrene-cyclopentane[48] and polystyrene-cyclohexane[49] solutions, respectively. The nature of these experimental systems suggests the use of Lennard-Jones (L-J) interactions in addition to the hard core potential acting between the monomers.

For infinitely long polymers, the monomer volume fraction, η, is zero at the critical point. Thus, the Θ temperature is defined by the following relation:

$$\left(\frac{\partial^2 P_b}{\partial \eta^2}\right)_\eta = 0 \tag{30}$$

With our GFD functional, this leads to $k_B\theta/\epsilon_{L-J} \approx 7.646$. Here, k_B is Boltzmann's constant, while ϵ_{L-J} is the usual L-J strength parameter. Under Θ conditions, the second-order density expansion of the interaction part of the free energy, predicts an infinite correlation length for a bulk solution of infinitely long polymers. This divergence is avoided, in our theory, by higher order density terms in the density functional.

We shall also assume that monomers are attracted to the surfaces via a L-J potential, eq 4, where the adsorption strength is determined by an amplitude parameter A_{L-J}. We shall maintain the pearl-necklace representation of the polymers.

A realistic polymer solution model should also capture the experimentally observed radius of gyration of the polymers. However, this criterion alone does not suffice to specify the monomer size (or bond length) and intrinsic chain rigidity (ϵ). We have therefore analyzed two model systems, both of which reproduces literature vales[47] of the radius of gyration for 6000-mers and 20000-mers, under Θ conditions. In one of our models, the chains are fully flexible, i.e., $\epsilon = 0$, and the monomers have a diameter of $\sigma = 6.6$ Å. The second model contains semiflexible chains, $\epsilon = 1$, while $\sigma = 4.8$ Å. We believe the latter model is the most realistic one because one would expect some local rigidity of the polymers due to the steric hindrance between phenyl groups. Furthermore, polystyrene has a bulk density of 1.07 g/cm^3,[49] and with $\sigma = 6.6$ Å, this corresponds to a reduced density of $n\sigma^3 = 1.85$, which by far exceeds cubic close packing! On the other hand, for the semiflexible chain model, $\sigma = 4.8$Å, giving $n\sigma^3 = 0.7$, which is a more reasonable value. Despite good argument to support the semiflexible model, the experimental data does not allow a unique specification of σ and ϵ. It is therefore reassuring that that our results using these two models are in close agreement (see below).

AK analyzed surface forces in the presence of 6000-mers and 20000-mers, respectively, at a polystyrene concentration of 15 μg/mL. This corresponds to bulk monomer concentrations of $n_b\sigma^3 = 0.000026$ and 0.00001, for our flexible and semiflexible polymer models, respectively. AK specifically focused on how these interactions respond to variations of the surface saturation. Undersaturated conditions were accomplished by allowing a short incubation period, following addition of polymer to the solution. Given our simplified model system, we are left with two unknown parameters, for the systems corresponding to "long incubation times". The unknowns are the surface potential strength, A_{L-J}, and the restricted diffusion threshold separation, h_T. Fortunately, as illustrated below, they have a rather weak influence on the surface interactions.

The experimental measurements, subsequent to long incubation times, displayed (see below) a rather long-ranged repulsion. Assuming that these conditions correspond to full surface saturation, the long range of the repulsion implies that the surfaces are covered by rather thick layers of polystyrene. Hence, we expect A_{L-J} to be strong enough to generate liquid-like monomer densities in the vicinity of the surfaces. On the other hand, physical arguments prevents the use of an adsorption potential minimum that is much deeper than one or two k_BT (per monomer). We shall use a reference value of $A_{L-J} = 5$, which gives a potential minimum of about $-1.4k_BT$. As we shall see below, the DFT predictions of our model systems underestimate the range of the surface interactions. In principle this might suggest that we have underestimated the surface affinity, as manifested by A_{L-J}. This is also supported by experimental adsorption values[47] of 2.5 ± 1.5 mg/m^2. This value, although of low accuracy, and based on certain assumptions, does seem to significantly exceed the corresponding calculated value, 0.6 mg/m^2, for 20000-mers and $A_{L-J} = 5$. However, the adsorption increases very slowly with A_{L-J}, and any physically reasonable value leads to a calculated adsorption which is smaller than the one quoted in the experimental work. The weak dependence of Γ_{eq} (as well as the range of the surface forces) on A_{L-J}, is demonstrated in Figure 10. Since the adsorption potential is rather short-ranged, the monomer density primarily respond in a narrow region close to the surfaces, when the surface potential parameter is increased. This largely corresponds to a flattening of adsorbed chains, and a 40 % increase of A_{L-J} only results in a 20 % increase of the calculated adsorption, to about 0.7 mg/m^2. This is also manifested in the surface interactions, where we see an increased amplitude of the forces, but with an almost constant range.

As in the experiments, we assume that the surfaces are able to absorb polymers (incubate) at wide slit widths. In our case, this corresponds to separations greater than or equal to h_T = 80 nm. We assume restricted equilibrium conditions apply below h_T, fixing the number of confined monomers per unit area to some prescribed value, $\Gamma = \int_0^{h_T/2} n(z)\, dz$. For very long incubation times, we expect that $\Gamma = \Gamma_{eq}$, where the latter quantity corresponds to the maximum adsorption allowed by equilibrium. It is of course possible that diffusion restrictions apply at even larger separations. In principle, this can be accounted for by choosing $\Gamma > \Gamma_{eq}$. However, Γ_{eq}, and thus the surface interaction, increase very weakly with h_T at such low monomer concentrations. This is due to the relatively rapid decay of the monomer density profiles, the range of which is determined by the radius of gyration, which is shorter than the bulk correlation length for the finite-sized polymers. However, for infinite polymers, the surface density profiles are governed by the bulk correlation length, rather than by the radius of gyration. At such low concentrations, the former is quite large and, in this case, Γ_{eq} displays a significant dependence on h_T. This is highlighted in Figure 11.

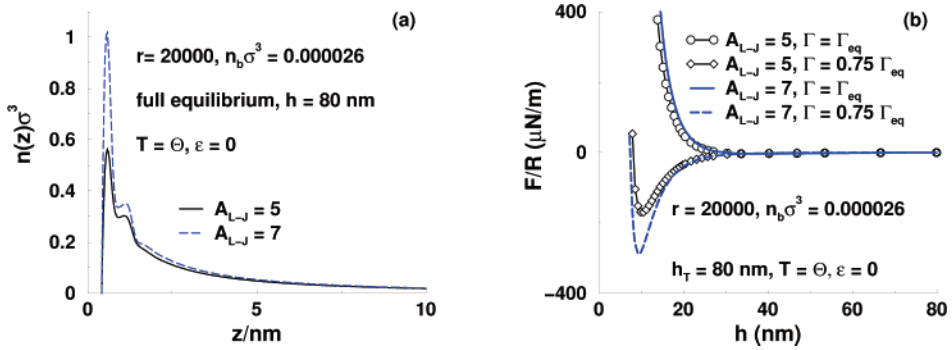

Figure 10. Responses to changes of the surface adsorption amplitude, A_{L-J}, for the fully flexible ($\epsilon = 0$) polymer model. Density functional predictions, for a model system with Lennard-Jones interactions. Below h_T, restricted equilibrium conditions apply, i.e., the number of confined monomers per unit area, 2Γ, is constant. We denote by $2\Gamma_{eq}$, the number of monomers per unit area, as obtained from full equilibrium calculations at a separation $h_T = 80$ nm. Key: (a) monomer density profiles; (b) surface interactions.

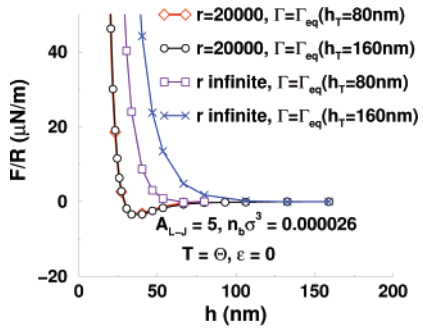

Figure 11. Responses to changes of h_T. The results are given for the fully flexible chain model, $\epsilon = 0$.

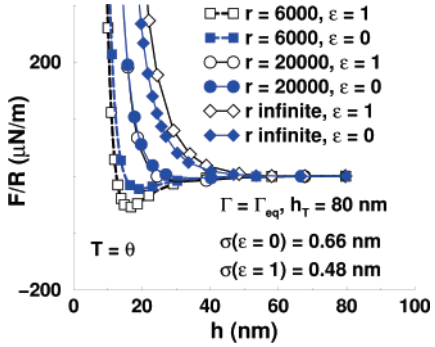

Figure 12. Comparing predicted surface interactions, using flexible ($\epsilon = 0$) and semiflexible ($\epsilon = 1$) polymer models, respectively.

Obviously, for the 20000-mers Γ_{eq}, and thus the surface interactions, are essentially independent of h_T in the regime beyond 80 nm. This is, however, not the case when the chains are infinite. The difference between finite and infinite chain behavior, in terms of dilution effects and the range of correlations, highlight the possible risks of using infinite chain theories to make predictions for polymers of finite length.

Before we proceed to experimental comparisons, we will demonstrate that our flexible and semiflexible polymer models lead to similar surface force predictions. In Figure 12, we have compared DFT predictions of surface interactions, assuming restricted equilibrium conditions, and full saturation at $h_T = 80$ nm. We see that predictions from the semiflexible chain approach are remarkably similar to corresponding ones with the fully flexible model. Hence, even though we believe the semiflexible model to be somewhat more realistic, this improvement has little impact on the predicted surface forces. On the other hand, this implies that the predictions are robust. Still, there are some differences to be noted. With short chains, the semiflexible model predicts more attractive interactions, having a slightly shorter range, than its flexible counterpart. In the presence of long chains, however, we find opposite qualitative differences.

3.2.2. Comparisons under Θ Conditions. The close agreement between predictions from either model allows us to limit ourselves to one of them, as we make experimental comparisons. Since we argue that our semiflexible model is the most realistic one, we will henceforth adhere to that choice.

In Figure 13, we have compared predictions and measurements of interactions in the presence of 20000-mers, including results from a 10000-fold dilution ($n_b\sigma^3 = 2.6 \times 10^{-9}$). Experimental data have been obtained from reference.[47] The qualitative response to dilution, as well as to undersaturation, is correctly reproduced by the theory, but the predicted interactions are more short-ranged than the corresponding measured ones. The experimental results indicate that the underestimation of polymer surface adsorption by the density functional theory, has a significant effect on the resulting surface forces. However, as discussed earlier, this is probably not due to an underestimation of A_{L-J} (or h_T). A more likely source is the possibility that there is another mechanism for a longer ranged force between surface polymer. For example, there is always some degree of ionic dissociation of the mica surface, even if the solution is a low dielectric fluid. If trace amounts of water are present, it will presumably accumulate at the surfaces and possibly impart a slight degree of surface dissociation. The presence of small amounts of water may have a profound influence on surface interactions in simple nonpolar liquids.[50] One may envisage a significant long-ranged tail in the monomer−surface adsorption potential, even if the surfaces only are only very weakly charged.

This notwithstanding, given that the model description itself is coarse-grained, the overall agreement is reasonably good. We also note that Ingersent et al.,[12] who modeled this system with a developed version of the deGennes density functional analysis,[3] underestimated the range and strength of the surface interactions by factors of 3.8 and 2.4, respectively.

It should be further noted, that experimental results also contradict each other. For example, measurements by Hu and Granick displayed a clear minimum under similar conditions (5100-mers), provided that the surfaces were approaching or receding slowly enough. In an earlier experiment,[49] on a polystyrene−cyclohexane solution at Θ conditions, a rather strong attractive interaction was found even after "long" incubation periods (6000-mers and 9000-mers), whereas Almog and Klein only found a monotonic repulsion (6000-mers and 20000-mers). The discrepancy between these experimental findings are, together with corresponding density functional

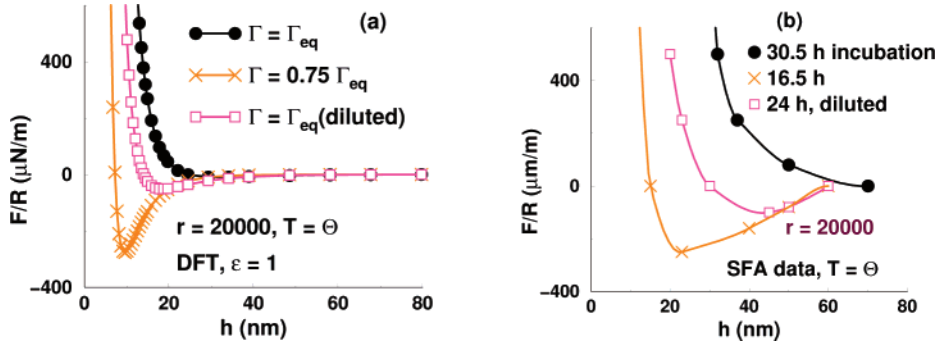

Figure 13. Interactions between mica surfaces, in the presence of a cyclopentane-polystyrene solution, at the Θ temperature. The chains are semiflexible, $\epsilon = 1$, and the monomer diameter is $\sigma = 4.8$ Å. The bulk monomer concentration is $n_b\sigma^3 = 0.00001$, except for the curves marked "diluted", which correspond to a 10000-fold dilution. (a) Density functional predictions. We reiterate that restricted equilibrium conditions apply below h_T. Here, the number of confined monomers per unit area, 2Γ, is constant. $2\Gamma_{eq}$ is the number of monomers per unit area, as obtained from full equilibrium calculations at a separation $h_T = 80$ nm. The curve indicated $\Gamma = 0.75\Gamma_{eq}$ thus corresponds to undersaturation, i.e., "short incubation time". (b) A rough reproduction, by simple "graph reading" (symbols), of Figure 8 in the work by Almog and Klein,[47] measuring interactions between mica surfaces immersed in a cyclopentane-polystyrene solution. The lines are obtained from a splines fit.

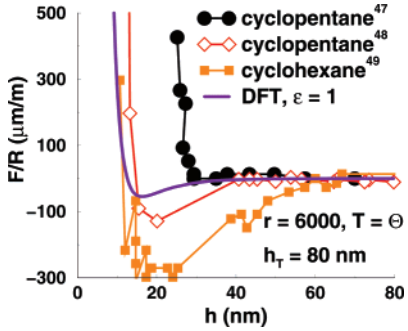

Figure 14. Interactions between mica surfaces at the Θ temperature. The polymer model is identical to that in Figure 13, except that the chains here are shorter: $r = 6000$. The experimental data have been reproduced from approximate readings of Figure 3 in ref 47, Figure 1 in ref 48, and Figure 3b in ref 49. These data were obtained for polystyrene dissolved in cyclopentane (refs 47 and 48) and cyclohexane (ref 49), respectively. In all cases, the measurements were claimed to be performed at "full saturation". The crosses display corresponding density functional predictions (DFT).

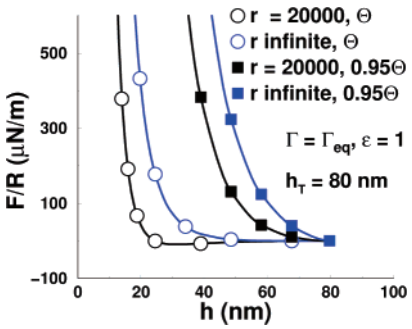

Figure 15. Responses to changes of the temperature (solvent quality).

predictions, illustrated in Figure 14. Strictly speaking, the experiments in ref 49 were performed at a slightly lower concentration, but the difference was too small to be of importance. Possibly more crucial is that these experiments were subsequent to similar ones at a lower temperature. It is unclear to us if the quoted incubation time (35 h) was conducted only at the Θ temperature. At any rate, the observed experimental differences may have several causes beyond those which can be addressed by a polymer solution theory.

3.2.3. Effects of Solvent Quality. Having evaluated the DFT under Θ conditions, we will now include a brief discussion on predicted and measured responses to changes of the temperature, i.e., to the solvent quality.

In Figure 15, we observe how the range of the surface forces increase with temperature, particularly as it drops below the Θ temperature. Long chains clearly display a strong response to temperature changes. It should be pointed out that $T = 0.95\Theta$ is below the critical temperature for 20000-mers. The temperature dependence is less drastic for short chains (not shown). The observed trend, for calculations below the Θ temperature, is in agreement with experimental findings by Hu and Granick,[48] although they found rather strong attractive interactions, in analogy with the results shown in Figure 14.

The large effect of small changes to the solvent quality suggests a possible source for the conflicting experimental findings. In particular, we note the significant increase of the range of the interactions in these systems (as predicted by the density functional theory). This suggests a much higher degree of polymer adsorption. Small amounts of impurities might change the solvent quality somewhat, and this can obviously have a strong influence on the observed forces. Experimentally measured forces are indeed sensitive to the presence of small amounts of other solvents.[51,52]

3.2.4. A Different Polymer Solution Model. We end these analyses by reporting some calculations based on modified density functional approach. utilizing a different set of assumptions than used in the model above. Specifically, we note that since we do not include solvent particles explicitly, we are implicitly adopting a McMillan−Mayer picture of the solution. This means, that provided we assume the polymer solution to be *globally* incompressible, we can directly relate the osmotic pressure to the solvent chemical potential. On the other hand, we allow the monomer density to attain any value locally. This is also the kind of model that is typically used in simulations. A different assumption is made in Flory−Huggins based theories, where the solutions is assumed to be *locally* incompressible, usually via a lattice description. We have developed a continuum density functional version of the Scheutjens−Fleer theory, which invokes local incompressibility. This means (see below) that the monomer density can never exceed the prescribed constant total density of the solution. Which is the best way to describe a polymer solution, using an implicit solvent approach? This is a very difficult question that cannot be answered by comparisons with simulations, unless these simulations include an explicit solvent. Even in the latter case, there is a risk that the results are sensitive to model parameters. It is of interest to see if the locally incompressible fluid (LIF) model will perform better than the "globally incompressible fluid" (GIF) density functional results above, when compared

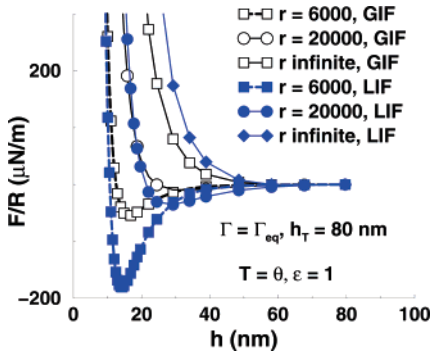

Figure 16. Comparing density functional predictions of implicit solvent polymer solution models, in which an assumption of *global*, GIF (eq 8), or *local*, LIF (eq 31) fluid incompressibility is assumed.

with experiments.

We obtain the LIF density functional model by rewriting the grand potential (eq 8) as

$$\beta\Omega[N(\mathbf{R})] = \beta F^{\mathrm{id}}[N(\mathbf{R})] + \int \{n_0 - n(z)\}\{\ln[n_0 - n(z)] - 1\}\,\mathrm{d}z + \beta F^{\mathrm{ex}} + \int \beta\{V_{\mathrm{ex}}(z) - \mu_{\mathrm{p}}\}n(z)\,\mathrm{d}z - \int \beta\mu_{\mathrm{s}}\{n_0 - n(z)\}\,\mathrm{d}z \quad (31)$$

where F^{ex} is a functional of the *local* total density, and μ_{s} is the chemical potential of the solvent. The total density, n_0, is constrained to be constant, i.e., F^{ex} is constant and the free energy can be considered a functional of the monomer density only. We have used the standard choice $n_0\sigma^3 = 1$, corresponding to cubic close packing.

The comparison is made, for our semiflexible chain model, in Figure 16. We see that the dependence on polymer length is more dramatic in the locally incompressible model. Still, given the scatter in experimental data, is it relieving to find such a good agreement between results from these different ways in which polymer solutions are modeled. It should be pointed out that it is easy to include spherical models of solvent molecules explicitly in the DFT. The disadvantage of such an approach is that the number of unknown parameters then increase even further.

4. Conclusions

We have studied the interaction free energy between two attractive surfaces, immersed in a polymer solution. We impose so-called "restricted equilibrium" conditions: beyond a certain cutoff separation, h_{T}, polymers are able to exchange freely between the bulk and the interstitial region. Below this separation, however, they are unable to diffuse in or out from the slit. A rich variety of possible interactions between surfaces is predicted by the density functional theory. The qualitative behavior of these surface forces is determined by parameters such as surface attraction, bulk monomer density, and chain length and stiffness, as well as the quality of the solvent.

As expected, restricted equilibrium interaction free energies are more repulsive, when compared with the full equilibrium case. Comparison between finite and infinite length polymers show a systematic increase in repulsion as the polymer length is increased, due primarily to the greater density of monomers present between the surfaces for the longer chains. The same trends are observed when the polymers are semiflexible. The surface repulsion increases with bulk monomer density and, at low enough concentrations, bridging forces generates a significant attractive regime.

The dependence of surface forces on the strength of the surface attraction is rather complex. A stronger surface affinity will naturally attract a larger number of polymers. This will strengthen the repulsive as well as the attractive contributions to the forces. Hence, the net outcome is nontrivial and nonmonotonic.

Hysteresis effects, observed in surface force experiments, can be mimicked by bringing the surfaces together under restricted equilibrium and allowing the system to reestablish equilibrium at short separations, before the surfaces are separated again under these new restricted equilibrium conditions.

It would be desirable to test these results against computer simulations. The simulations would pose fewer difficulties compared with the full equilibrium systems. In the latter systems, performing exchanges with a bulk are problematic due to the high probability of polymer−polymer overlap.

The latter part of this work contains experimental comparisons. In this case, potentials of mean force between the species can only be roughly estimated. Nevertheless, the Θ condition reduces the number of independent thermodynamic variables. We have demonstrated that our density functional theory reproduces the same qualitative response to changes of undersaturation, as well as to dilution and temperature change. The range of the surface forces appears to be underestimated, but there are also significant discrepancies between experiments conducted under seemingly similar conditions. A plausible explanation of the underestimated range, is that we have assumed monodisperse samples. In a polydisperse solution, long chains will be preferentially adsorbed at the surfaces. This suggests a dominance of the large molecular weight tail of the chain length distribution, i.e., more long-ranged interactions than implied by the average degree of polymerization. Another possible source of the discrepancy is that while our theoretical approach always monitors the free energy minimum, subject to the imposed constraints, measured surface interactions may suffer from nonequilibrium effects. Specifically, it is possible that bridge formation is suppressed by large free energy barriers, as two saturated surfaces approach. With undersaturated surfaces, it is presumably easier for adsorbed chains to find "open spots" on the adjacent surface. Such behaviors can in principle be handled by the density functional approach, by imposing further restrictions. One could, for instance, limit the number of acceptable configurations to those where the chain ends are on the same side of the mid plane between the surfaces. This might be a plausible model for the case of saturated surfaces. The problem is how to unambiguously allow for bridge formation at undersaturated conditions.

The range of the surface interactions are, for long chains, dramatically increased when the solvent quality is just slightly poorer than under Θ conditions. Hence, small amounts of impurities can have a significant influence on the measured forces. This might be one of the reasons why experimental results deviate, even for systems that are very similar.

An important finding in this study is that the predicted surface interactions are insensitive to "reasonable" changes of parameters that we have little knowledge about, e.g., intrinsic chain stiffness and surface potential strength. We have also noted that the infinite chain length version of the DFT is useful, with very rapid numerical solutions. Still, one has to be careful when interpreting the predictions, especially when the bulk monomer concentration is low. In those cases, there are some qualitative behaviors that only can be captured by treating the finite size of polymers properly.

Acknowledgment. J.F. thanks the Swedish Science Council for financial support.

References and Notes

(1) Horn, R. G.; Hirz, S. J.; Hadziioannou, G.; Frank, C. W.; Catala, J. M. *J. Chem. Phys.* **1989**, *90*, 6767.
(2) Taunton, H. J.; Toprakcioglu, C.; Fetters, L. J.; Klein, J. *Macromolecules* **1990**, *23*, 571.
(3) deGennes, P. G. *Macromol.* **1982**, *15*, 492.
(4) Klein, J. *J. Chem. Soc. Faraday Trans. I* **1983**, *79*, 99.
(5) Scheutjens, J. M. H. M.; Fleer, G. J. *Macromolecules* **1985**, *18*, 1882.
(6) Woodward, C. E.; Forsman, J. *Phys. Rev. E* **2006**, *74*, 010801.
(7) Edwards, S. F. *Proc. R. Soc. London* **1965**, *85*, 613.
(8) deGennes, P. G. *Rep. Prog. Phys.* **1969**, *32*, 187.
(9) Joanny, J.-F.; Leibler, L.; deGennes, P. G. *J. Polym. Sci.: Polym. Phys. Ed.* **1979**, *17*, 1073.
(10) deGennes, P. G. *Macromolecules* **1981**, *14*, 1637.
(11) Klein, J.; Pincus, P. *Macromolecules* **1982**, *15*, 1129.
(12) Ingersent, K.; Klein, J.; Pincus, P. *Macromolecules* **1990**, *23*, 548.
(13) Semenov, A. N. *J. Phys. II* **1996**, *6*, 1759.
(14) Bonet-Avalos, J.; Joanny, J.-F.; Johner, A.; Semenov, A. N. *Europhys. Lett.* **1996**, *35*, 97.
(15) Woodward, C. E. *J. Chem. Phys.* **1991**, *94*, 3183.
(16) Woodward, C. E.; Yethiraj, A. *J. Chem. Phys.* **1994**, *100*, 3181.
(17) Dijkstra, M.; Frenkel, D.; Hansen, J. P. *J. Chem. Phys.* **1994**, *101*, 3179.
(18) Forsman, J.; Woodward, C. E.; Freasier, B. C. *J. Chem. Phys.* **2002**, *117*, 1915.
(19) Forsman, J.; Woodward, C. E. *Phys. Rev. Lett.* **2005**, *94*, 118301.
(20) Forsman, J.; Woodward, C. E. *Phys. Rev. E* **2006**, *73*, 051803.
(21) Luna-Barcenas, G.; Bennet, G. E.; Sanchez, I. C.; Johnston, K. P. *J. Chem. Phys.* **1998**, *104*, 9971.
(22) Luna-Barcenas, G.; Meredith, J. C.; Sanchez, I. C.; Johnston, K. P. *J. Chem. Phys.* **1998**, *107*, 10782.
(23) Gromov, D. G.; de Pablo, J. J.; Luna-Barcenas, G.; Sanchez, I. C.; Johnston, K. P. *J. Chem. Phys.* **1998**, *108*, 4647.
(24) Chhajer, M.; Guijrati, P. D. *J. Chem. Phys.* **1998**, *109*, 9022.
(25) Forsman, J.; Woodward, C. E. *J. Chem. Phys.* **2003**, *119*, 1889.
(26) Semenov, A. N.; Joanny, J.-F.; Johner, A.; Bonet-Avalos, J. *Macromolecules* **1996**, *30*, 1479.
(27) Blokhuis, E. M.; Skau, K. I. *J. Chem. Phys.* **2003**, *119*, 3483.
(28) Nordholm, S.; Johnson, M.; Freasier, B. C. *Aust. J. Chem.* **1980**, *33*, 2139.
(29) Honnell, K. G.; Hall, C. K. *J. Chem. Phys.* **1991**, *95*, 4481.
(30) Yu, Y.-X.; Wu, J. *J. Chem. Phys.* **2002**, *117*, 2368.
(31) Turesson, M.; Forsman, J.; Åkesson, T. *Phys. Rev. E* **2007**, *76*, 021801.
(32) Åkesson, T.; Woodward, C. E.; Jönsson, B. *J. Chem. Phys.* **1989**, *91*, 2461.
(33) Wichert, J. M.; Gulati, H. S.; Hall, C. K. *J. Chem. Phys.* **1996**, *105*, 7669.
(34) Forsman, J.; Broukhno, A.; Jönsson, B.; Åkesson, T. *J. Chem. Phys.* **2004**, *120*, 413.
(35) Forsman, J.; Woodward, C. E. *J. Chem. Phys.* **2004**, *120*, 506.
(36) Forsman, J.; Woodward, C. E. *Macromolecules* **2006**, *39*, 1269.
(37) Wertheim, M. S. *J. Chem. Phys.* **1987**, *87*, 7323.
(38) Chiew, Y. C. *Mol. Phys.* **1990**, *70*, 129.
(39) Song, Y.; Lambert, S. M.; Prausnitz, J. M. *Macromolecules* **1994**, *27*, 441.
(40) Chang, J.; I.; S. S. *J. Chem. Phys.* **1995**, *103*, 3196.
(41) Forsman, J.; Woodward, C. E.; Freasier, B. C. *J. Chem. Phys.* **2003**, *118*, 7672.
(42) Scheutjens, J. M. H. M.; Fleer, G. J. *J. Phys. Chem.* **1979**, *83*, 1619−1635.
(43) Woodward, C. E.; Forsman, J. *Macromolecules* **2004**, *37*, 7034.
(44) Forsman, J.; Woodward, C. E. *Macromolecules* **2006**, *39*, 1261.
(45) Ingersent, K.; Klein, J.; Pincus, P. *Macromolecules* **1986**, *19*, 1375.
(46) Klein, J.; Rossi, G. *Macromolecules* **1998**, *31*, 1979.
(47) Almog, Y.; Klein, J. *J. Colloid Interface Sci.* **1985**, *106*, 33.
(48) Hu, H.-W.; Granick, S. *Macromolecules* **1990**, *23*, 613.
(49) Israelachvili, J.; Tirrell, M.; Klein, J.; Almog, Y. *J. Colloid Interface Sci.* **1985**, *106*, 33.
(50) Christensson, H. K. *J. Colloid Interface Sci.* **1985**, *104*, 234.
(51) Marra, J.; Christensson, H. K. *J. Phys. Chem.* **1989**, *93*, 7180.
(52) Guzonas, D. A.; Hair, M. L. *Langmuir* **1991**, *7*, 2346.

MA071181T